

Copyright 2021, ICC & ABRACO

The work presented during 21st INTERNATIONAL CORROSION CONGRESS & 8th INTERNATIONAL CORROSION MEETING in the month of July of 2021.

The information and opinions contained in this work are of the exclusive right of the author(s).

Poster Oral

A decisão final será do Comitê Técnico.

Guanine as an Environmentally Friendly Corrosion Inhibitor for Copper and X65 Steel Surfaces in HCl Solution – An Electrochemical and Raman Investigation

Elaine F. Silva^a, Julio S. Wysard^b, Maria J. M. Andrade^c, Tatiana C. Almeida^{a,d}, Merlin C. E. Bandeira^a, Oscar R. Mattos^e.

Abstract

Inhibition of copper and X65 steel corrosion by Guanine in HCl 0.1 mol.dm⁻³, pH = 2.0, solutions were investigated by a combination of electrochemical and weight loss experiments as well as Raman spectroscopy. Electrochemical results revealed that Guanine adsorption modifies the copper surface, inhibiting its dissolution in the tested medium and weight loss experiments showed an 87 % inhibition efficiency (IE). A much smaller IE was determined for X65 steel via weight loss experiments (IE = 22%) and the low protection offered by Guanine towards steel corrosion in HCl solution was corroborated by cyclic voltammetry and potentiodynamic polarization data. Spectroscopic results showed that the neutral Guanine species is present on both metal surfaces, because of the loss of a hydrogen ion from the GuanineH⁺ upon adsorption. The neutral species reacts with Cu(I) ions, resulting in a Cu(I)Guanine compound that forms an insoluble and adherent layer, effectively protecting the metal surface. The much lower IE of Guanine towards X65 steel corrosion can be explained by the formation of a non-adherent iron-Guanine compound.

Keywords: Corrosion Inhibitor, Guanine, HCl, Copper, X65 Steel.

Introduction

Corrosion of metallic materials is a recurrent problem in many industrial segments and the use of corrosion inhibitors is one of the most common and efficient strategies to mitigate it [1,2]. Indeed, copper is widely used in water supply and heat exchanging systems and the X65 steel is one of the most relevant materials in the petrochemical industry [3,4]. Both materials are exposed to highly acidic solutions during service, stressing the need to employ efficient corrosion inhibitors to avoid major metal loss. As a matter of fact, copper shells on heat exchangers require periodic pickling and descaling that is usually carried out with either HCl or H₂SO₄ solutions [5-7]. The direct involvement of chloride anions on the copper electrodisolution mechanism leads to formation of a porous CuCl layer that is continually being dissolved by attack of further chloride ions, giving CuCl₂⁻, that is soluble and diffuses to

^a PhD, Materials and Metallurgical Engineering – LNDC-COPPE-UFRJ

^b M.Sc., Chemistry – IQ-UFRJ

^c Undergraduate Student – Metallurgical Engineering – UFF

^d Prof. Metallurgical Engineering – VMT-UFF

^e Prof. Metallurgical Engineering – LNDC-POLI-COPPE-UFRJ

the bulk solution, leaving the metal surface unprotected [8,9]. X65 steel is exposed to HCl solutions during the acidification procedure, that aims at improving oil production [10]. So, it becomes very important to characterize the interaction and inhibition efficiency (IE) of corrosion inhibitors for both materials in hydrochloric acid medium.

Due to the growing ecological awareness as well as the strict environmental regulations being adopted worldwide, acceptable corrosion inhibitor candidates should prevent metal dissolution and be compatible with the environment. Additionally, inhibitor formulations containing toxic compounds, such as chromate or benzotriazole, should be replaced by less harmful alternatives [11]. These environmental demands have led researchers to focus on organic molecules containing both heteroatoms (N, O, P, S atoms) and conjugated π systems as possible low-toxicity inhibitors for metals in different corrosive media. In this context, Imidazole and its derivatives have been widely investigated in the inhibition of copper and iron corrosion in chloride media, with inhibition efficiency (IE) results being affected by solution composition, pH, temperature and inhibitor chemical structure. Recent literature results revealed that the derivatives containing either aromatic or anchoring groups like -SH or -RCOOR' and others have shown better performance [5-7]. Guanine (Fig. 1) is an aryl-substituted imidazole derivative, that has multiple adsorption sites, and can be found in low concentration in surface waters as well as in plant and animal tissues. Being one of purine bases of the nucleic acids (DNA and RNA), Guanine is non-toxic and easily removed from waste waters by acid hydrolysis. It is also used as an industrial additive to cosmetics and other products as a white pigment or to provide luster [12-16]. Its use as a corrosion inhibitor is far more recent and still not widespread, once Guanine has been tested in a small number of metal surfaces and corrosive media. For instance, Tao *et al.* [15] investigated Guanine as a copper corrosion inhibitor for H_2SO_4 0.5 mol.dm^{-3} solution by potentiodynamic polarization, electrochemical impedance, and weight loss experiments. Their results showed that Guanine acts as a mixed-type inhibitor, and that its IE increased with inhibitor concentration to a maximum of 92% at $0.001 \text{ mol dm}^{-3}$. Weight loss data obtained after 6 hours of immersion, were used to calculate $\Delta G^{\circ}_{\text{ads}}$, that pointed to a physisorption mechanism. A much smaller IE of Guanine was found by Yan *et al.* [13] for mild steel immersed in 1.0 mol.dm^{-3} HCl solutions. Electrochemical and weight loss results showed that Guanine also behaves as a mixed-type corrosion inhibitor and that its IE increases with the purine concentration up to 68% at $0.001 \text{ mol.dm}^{-3}$. Implantation of amino or mercapto groups on the Guanine ring resulted in increased inhibition performance for this class of molecules. Quantum chemical calculations performed for the isolated molecules related their IE to the energy gap of the frontier orbitals ($\Delta E_{\text{HOMO-LUMO}}$) and based on the lack of correlation between IE values and the energies of each frontier orbital, the authors proposed that Guanine and its derivatives physisorb on the steel surface. Finally, Chahul *et al.* [14] obtained similar results to Yan *et al.* [13] concerning Guanine inhibition of mild steel corrosion in H_3PO_4 0.1 mol.dm^{-3} media.

Adsorption of Guanine on copper has also been characterized by different spectroscopic techniques. Yamada *et al.* [17] used infrared reflection absorption spectroscopy (IRRAS) in the characterization of DNA nitrogen bases and the Cu(110) surface in ultrahigh vacuum. Their results showed that the Guanine molecule adsorbed on the copper single crystal by the $\text{R-N}_1\text{H-C}_6=\text{O}$ site, resulting in a tilted configuration. Furukawa *et al.* [18] employed X-ray photoelectron (XPS) and near-edge X-ray fine structure absorption (NEXAFS) spectroscopies to determine that Guanine was deprotonated at N_1 upon adsorption on the Cu(110) surface and that the anion also adsorbed in a tilted orientation with respect to the single-crystal. Density functional theory (DFT) calculations confirmed the spectroscopic results, showing that the lowest energy configuration was attained when deprotonated Guanine adsorbed on copper employing its N_1 and O atoms. A scanning tunnelling microscopy (STM) investigation of

Guanine adsorption on Cu(111) performed at low temperature (~80 K) revealed that Guanine adsorbs flatly on the metal surface, forming an ordered superstructure comprised of hydrogen-bonded purine molecules [19], contrary to the tilted structures derived from spectroscopic techniques. To the best of our knowledge, adsorption of Guanine on copper has not been characterized by Surface Enhanced Raman Spectroscopy (SERS), that is a special Raman technique that allows assessment of the *in situ* spectrum of an adsorbed monolayer on properly roughened coinage metal surfaces, or even by Raman spectroscopy itself. Besides that, we were not able to find any spectroscopic investigation on the Guanine interaction with either iron or steel surfaces.

Based on that, we carried out an electrochemical and Raman investigation of Guanine adsorption and inhibition efficiency towards copper and X65 steel corrosion in HCl 0.1 mol.dm⁻³ solutions, aiming at elucidating the behavior of this molecule towards these chemically different and very important metallic materials.

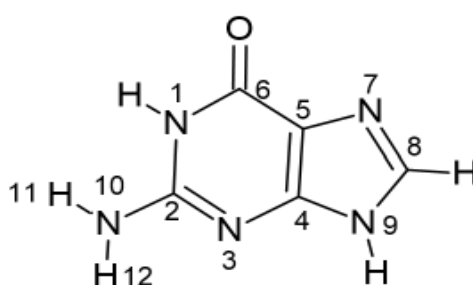


Figure 1 – Guanine molecular structure and atom numbering scheme.

Methodology

Guanine solutions ($c = 0.001 \text{ mol.dm}^{-3}$) were prepared by dissolving the corresponding amount of the solute in the required volume of concentrated HCl to make 0.1 mol.dm^{-3} . Then deionized water was added to complete 1 dm^{-3} of solution, followed by vigorous stirring. After preparation, the pH of the solutions was adjusted to 2.0 with concentrated NaOH and HCl, if needed. Hereafter, Guanine containing HCl solutions will be referred to as Guanine solutions only, leaving the presence of the acid implicit. The concentration of $0.001 \text{ mol.dm}^{-3}$ of Guanine equals the solubility limit for this compound in aqueous solution at $\text{pH} = 2.0$ and this is reported to be the optimal Guanine concentration to achieve maximum inhibition efficiency for the protection of both copper and steel surfaces in acidic media [13-15]. Experiments were carried out for less concentrated Guanine solutions and smaller inhibition efficiencies were observed [20], so we decided to work only with the $0.001 \text{ mol.dm}^{-3}$ concentration.

Electrochemical measurements were carried out in a conventional three electrode cell, using a rotating disc electrode (RDE) apparatus where the working electrode was either a polycrystalline copper rod (area = 0.2 cm^2) or a X65 steel rod embedded in epoxy resin (area = 0.16 cm^2). A platinum grid and a saturated calomel electrode (SCE) were employed as counter and reference electrodes, respectively. All potentials are quoted to SCE scale and a rotation speed of 1000 rpm was selected to all electrochemical experiments. Cyclic voltammetry and potentiodynamic polarization experiments were carried out after stabilization of the open circuit potential (OCP) at sweep rates of 0.01 V.s^{-1} and $0.000125 \text{ V.s}^{-1}$, respectively. The initial potential for the cyclic voltammetry was chosen in order to avoid evolution of hydrogen gas at

the beginning of the experiment. Weight loss experiments were performed by immersion of test coupons in either HCl 0.1 mol.dm^{-3} or Guanine $0.001 \text{ mol.dm}^{-3}$ solution, pH = 2.0, at room temperature ($298 \pm 2 \text{ K}$). Prior to immersion, the samples of $12 - 14 \text{ cm}^2$ area were mechanically cleaned with emery papers of different mesh up to 600 mesh finish. Then, they were washed with deionized water, degreased with acetone in an ultrasonic bath and finally dried in airflow. The ratio of solution volume to specimen area was kept at $30 - 40 \text{ mL.cm}^{-2}$ to minimize pH changes during immersion time and the tests were stopped as soon as any pH changes were detected. After immersion, the samples were cleaned in the appropriate solutions, dried and weighed. The cleaning procedure was repeated until constant weight and all measurements were made in triplicate, according to ASTM G1 [21].

Raman spectrum of solid Guanine was acquired with a Bruker SENTERRA confocal Raman microscope, using the 532 nm excitation line with 10 mW of power focalized on the sample by a 20x long working distance objective (Olympus). The sample was accommodated in a microscope slide and 3 coadditions of 30 s were collected with $3 - 5 \text{ cm}^{-1}$ resolution. Surface enhanced Raman spectra (SERS) of a $0.001 \text{ mol.dm}^{-3}$ Guanine at pH = 2.0 were acquired in a three-electrode electrochemical cell, with a copper working electrode of 0.2 cm^2 of area, a platinum grid and a SCE as counter and reference electrodes, respectively. Spectra were obtained as function of applied potential and immersion time using the 785 nm line of excitation, with 25 mW of power. Integration time was set to 10 s that were coadded 3 times to produce spectra with good signal-to-noise ratio. A potential window of -1.0 to +0.4 V was selected, and spectra were recorded with 0.1 V intervals, after stabilization of the OCP. Pre-treatment and activation procedures of the working electrode were detailed elsewhere [22,23]. SERS spectra of Guanine adsorbed on X65 steel could not be acquired since iron is not an appropriate material to sustain surface plasmon resonance in the conditions used in this work [24], so normal Raman spectra were acquired from X65 coupons withdrawn from Guanine solutions after weight loss experiments. These spectra were acquired using the same acquisition conditions employed to obtain the spectrum of the solid purine sample.

Results and Discussion

Inhibition of Copper Corrosion by Guanine

Cyclic voltammograms acquired for the copper electrode immersed in both blank and $0.001 \text{ mol.dm}^{-3}$ Guanine solutions can be seen in Fig. 2. The onset of copper dissolution in HCl 0.1 mol.dm^{-3} (Fig. 2 – black line) is observed at $E = -0.125 \text{ V}$ followed by the broad peak extending from $E = 0.0$ to 0.3 V , assigned to the $\text{CuCl}/\text{CuCl}_2^-$ formation, and a current increase until $E = 0.4 \text{ V}$, that is attributed to continued metal dissolution as both CuCl and CuCl_2^- [22,23]. These species are subsequently reduced at the cathodic sweep, where peaks at $E = -0.10$ and -0.31 V can be seen. Reduction of hydrogen is observed at $E \leq -0.7 \text{ V}$ [22,23]. Addition of Guanine to the corrosive medium leads to changes in the voltammogram of the copper electrode (Fig. 2 – red line). The onset of copper dissolution remains unaltered, but a much narrower peak, centered at $E = 0.19 \text{ V}$, can be observed in the anodic sweep. The anodic current obtained at $E = 0.4 \text{ V}$ is 17.8 mA, a value significantly smaller than the 26.1 mA observed at the same potential for the blank HCl solution. The peak at $E = -0.1 \text{ V}$ was suppressed and the main cathodic peak is shifted to $E = -0.33 \text{ V}$, with -15 mA of current compared to -18.6 mA obtained for neat HCl media. Besides that, the onset of hydrogen reduction shifts to $E = -0.8 \text{ V}$ in contrast to the neat HCl solution, having lower current densities in the presence of the purine. These results show that adsorption of Guanine molecules on copper modifies the electrode surface,

making the formation of CuCl and CuCl_2^- and the reduction of H^+ more difficult. The increase in the cathodic current of the peak at $E = -0.33$ V and its broadening in the voltammogram of $0.001 \text{ mol.dm}^{-3}$ Guanine solutions may indicate that the purine molecules react with the corrosion products, forming a new entity that is reduced at the cathodic sweep.

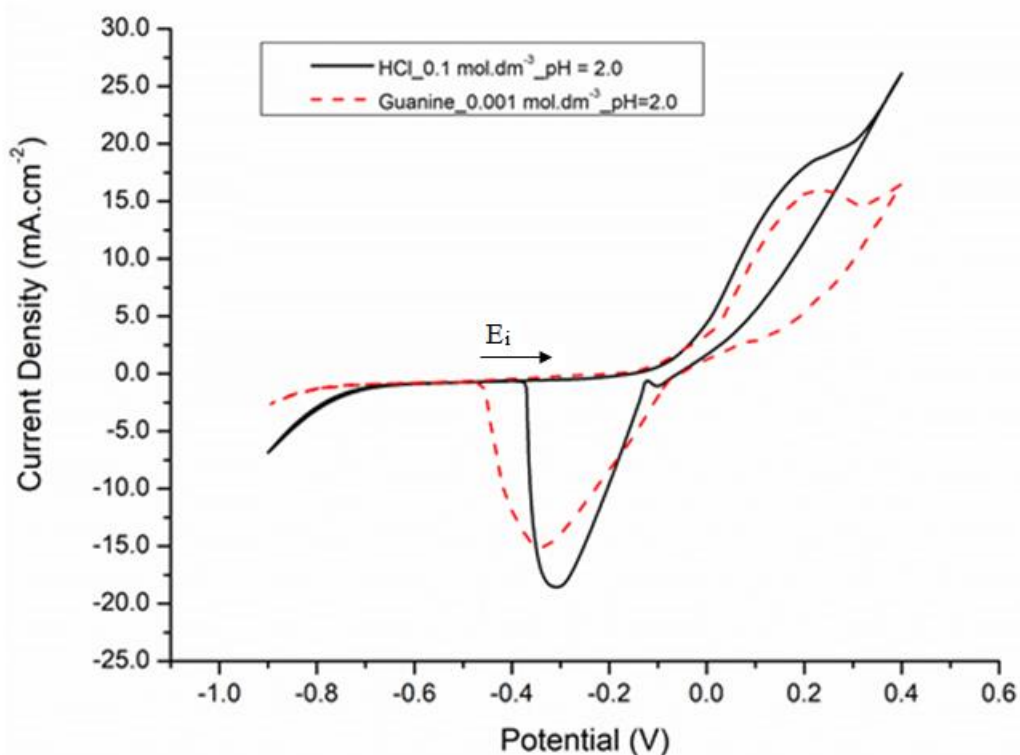


Figure 2 – Voltammograms obtained for the copper electrode immersed in HCl 0.1 mol.dm^{-3} (black line) or Guanine $0.001 \text{ mol.dm}^{-3}$ (red line) at pH = 2.0.

Potentiodynamic polarization curves were obtained for the copper electrode immersed in either neat HCl solution or Guanine containing solution and the results are displayed in Figure 3. One can see that only the anodic branch of the polarization curve, obtained between the OCP and $+0.4$ V vs OCP, is shown in Fig. 3. The reasoning behind this choice is that the cathodic branch of the curve is essentially the same in both solutions, so we decided to discuss only the anodic features, that are far more relevant. Analysis of the polarization curve obtained for the blank solution shows that the current density increases steadily as the potential is made more positive, until $E = 0.025$ V, where a small peak can be seen. This peak is assigned to the formation of the CuCl film, which is partially dissolved as CuCl_2^- when the potential is made more positive [25]. Therefore, the current continues to increase, and a current plateau cannot be seen.

A quite different polarization curve is obtained when Guanine is present in the corrosive medium, where it becomes possible to identify three different regions in the E vs $\log(i/A)$ plot: (i) OCP to $E = -0.1$ V; (ii) $E = -0.1$ to -0.025 V and (iii) -0.025 V to $E = 0.21$ V. In the first region, the current increases rapidly with increasing anodic polarization, meaning that copper is in active dissolution regime. In the intermediate region, the current increases more slowly with applied potential and a change in the slope of the curve is clearly seen. As a matter of fact, at the same potential region, slopes of 81 and 180 mV/dec are calculated for the blank and 0.001

mol.dm⁻³ Guanine solutions, respectively. Such a different behavior can be interpreted in terms of Guanine adsorption on the copper electrode, modifying its surface and making Cl⁻ attack more difficult. At the third potential region, a well-resolved peak can be seen at E = 0.0 V, followed by a current plateau, where current values are one order of magnitude smaller than the ones observed for the neat HCl solution. It is worth mentioning that the copper electrode was covered by a white layer at the end of the experiment. Formation of an insoluble white compound, generally referred to as a Cu(I)Guanine complex of unidentified stoichiometry was observed at E ≈ 0.0 V [26]. Based on that, we assigned the peak observed at E = 0.0 V in this work to the formation of a Cu(I)Guanine compound, that eventually forms a protective layer on the metal, partially blocking the surface from the aggressive Cl⁻ anions. Characterization of the stoichiometry and chemical structure of this compound is currently underway.

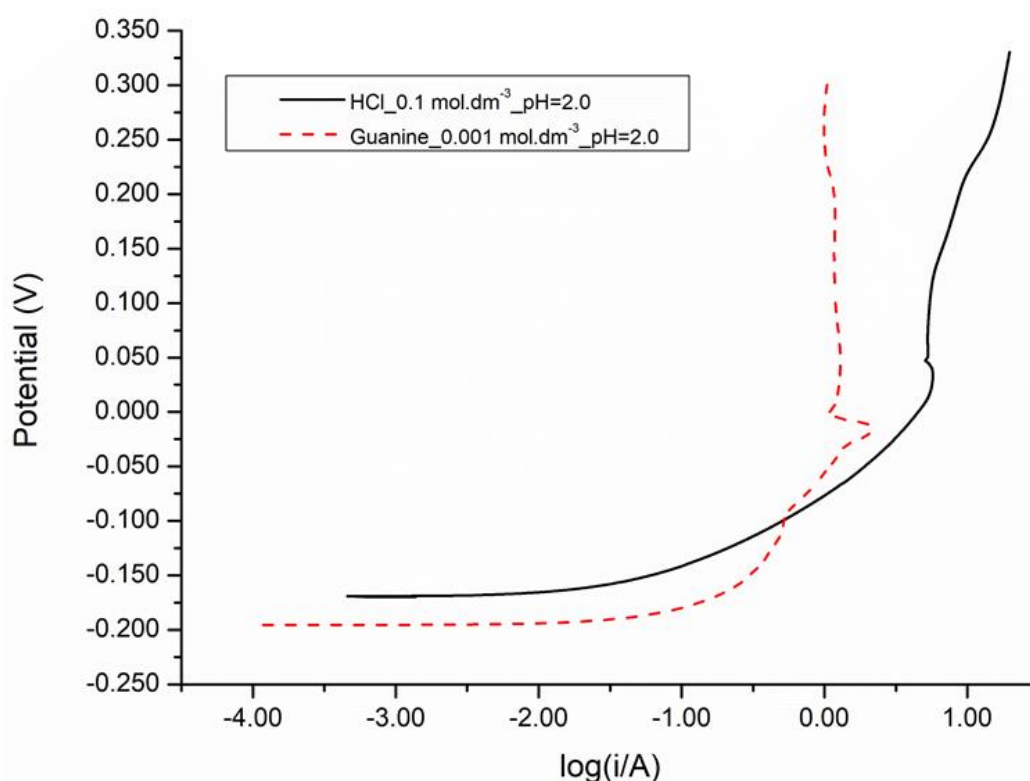


Figure 3 – Potentiodynamic polarization curves obtained for a copper electrode immersed in either HCl 0.1 mol.dm⁻³ or Guanine 0.001 mol.dm⁻³, at pH = 2.0.

The electrochemical results presented here revealed that Guanine can inhibit copper corrosion in HCl solutions, but these results are limited to a small time interval. It is desirable to know whether the protection offered by the purine is maintained at higher immersion times. Based on that, weight loss experiments were carried out to investigate this hypothesis and to quantify the inhibition efficiency (IE) of Guanine. Results obtained for the copper coupons immersed for 90 hours in both blank and inhibited solutions can be seen in Table 1.

One can easily see that when Guanine is added to the corrosive medium, the weight loss per area is greatly reduced, from 0.0141 g.cm⁻² in the blank solution to 0.0019 g.cm⁻², giving an inhibition efficiency (IE) of 87%. Visual inspection of the copper coupons withdrawn from the inhibited solution showed a thick and adherent white layer, that could only be removed by a combination of chemical cleaning and mechanical abrasion. Scanning electron microscopy (SEM) revealed that a film of Cu(I)Guanine, composed of long and thin “thread-like” structures, covered the copper coupon that was exposed to the purine solution while the metal

sample immersed in neat HCl presented an irregular rough surface with CuCl crystals on it (Fig. 4). Measurement of the film thickness carried out in SEM images showed that the film is 25 – 40 μm thick. Based on these results, it is possible to conclude that the thick, uniform, and adherent Cu(I)Guanine film is the reason behind the high efficiency offered by this inhibitor.

Table 1 – Average weight loss calculated for copper samples immersed for 90 h in HCl solutions (pH = 2.0) containing or not Guanine.

Solution	Weight loss/area ($\text{g}\cdot\text{cm}^{-2}$)	Inhibition Efficiency (%)
HCl 0.1 $\text{mol}\cdot\text{dm}^{-3}$	0.0141	-
Guanine 0.001 $\text{mol}\cdot\text{dm}^{-3}$	0.0019	87

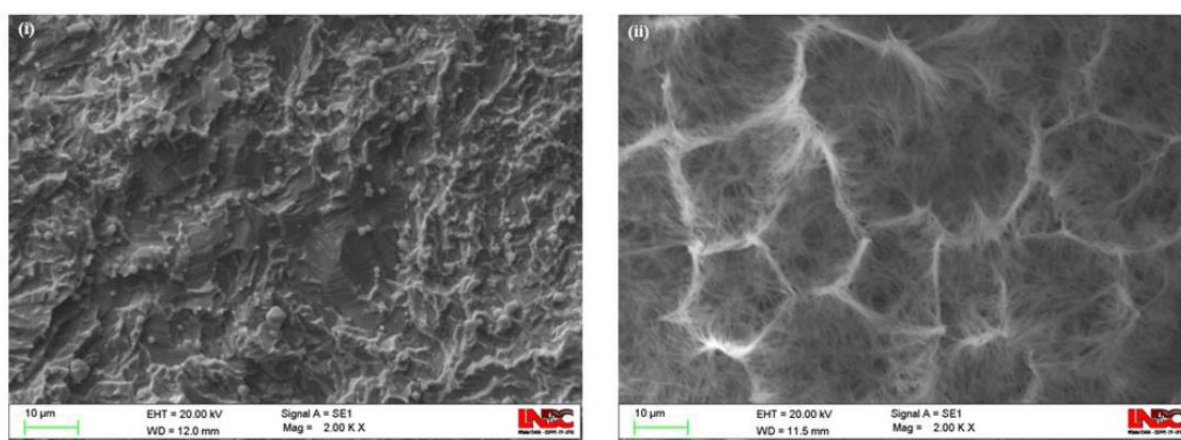


Figure 4 - Scanning electron micrographs obtained for copper samples immersed in both blank HCl (a) and 0.001 mol L⁻¹ Guanine (b) solutions for 90 h.

Electrochemical and weight loss experiments provide macroscopic information concerning the adsorption and inhibition efficiency of a molecule, but they cannot bring insight on the specific molecule-surface bonding, molecular orientation upon adsorption and other microscopic information, so we decided to acquire Surface Enhanced Raman Spectra (SERS) of Guanine solutions on a copper electrode, as copper is an adequate substrate to acquire SERS spectra with visible light excitation [24]. Figure 5 shows the normal Raman spectrum (NRS) of solid Guanine and the SERS spectra of the same molecule adsorbed on a copper electrode from a 0.001 mol L⁻¹ solution, pH = 2.0, at the OCP. Characteristic wavenumbers and assignments of the most intense Guanine bands can be found in Table 2.

Analysis of the surface spectrum of adsorbed Guanine is quite similar to the NRS of the solid purine and its SERS spectrum acquired on Ag colloids or electrodes at pH = 5.0 solutions [27,28]. This resemblance may be interpreted as evidence of adsorption of the neutral Guanine molecule on the copper electrode, a hypothesis that is supported by the lack of characteristic GuanineH⁺ bands [29] on the SERS spectra of Fig. 5. Adsorption of the neutral species may seem unlikely because of the high acidity of the solution. Indeed, the equilibrium between the monoprotonated (GuanineH⁺) and neutral Guanine has $\text{pK}_a = 3.3$, so at pH = 2.0, about 95% of the molecules in the bulk solution are protonated [30]. However, adsorption can reduce the pK_a determined for bulk reactions as shown by Oh *et al.* [31], that could only observe the adsorption of protonated Guanine on Ag sols at pH ≤ 1.0 . Based on this rationale, adsorption of neutral

Guanine on the copper electrode may be explained by the initial interaction of the protonated form with the metal, that resulted in a decrease of its pK_a and ultimately in the loss of a H^+ ion. Besides the Guanine bands, an intense band located at 298 cm^{-1} is assigned to ν_{CuCl} mode of the CuCl film [22,23], meaning that a CuCl film is initially formed on the copper electrode despite Guanine adsorption. Finally, intensification of in-plane modes (A') and the appearance of a copper-nitrogen stretching mode (ν_{CuN}) at 320 cm^{-1} in the SERS spectrum of Guanine acquired on a copper electrode at $E = -0.9\text{ V}$ (not shown) reveal that the molecule chemisorbs on the metal in an upright or slightly tilted configuration. The spectral pattern is consistent with adsorption via N_3 [28,32].

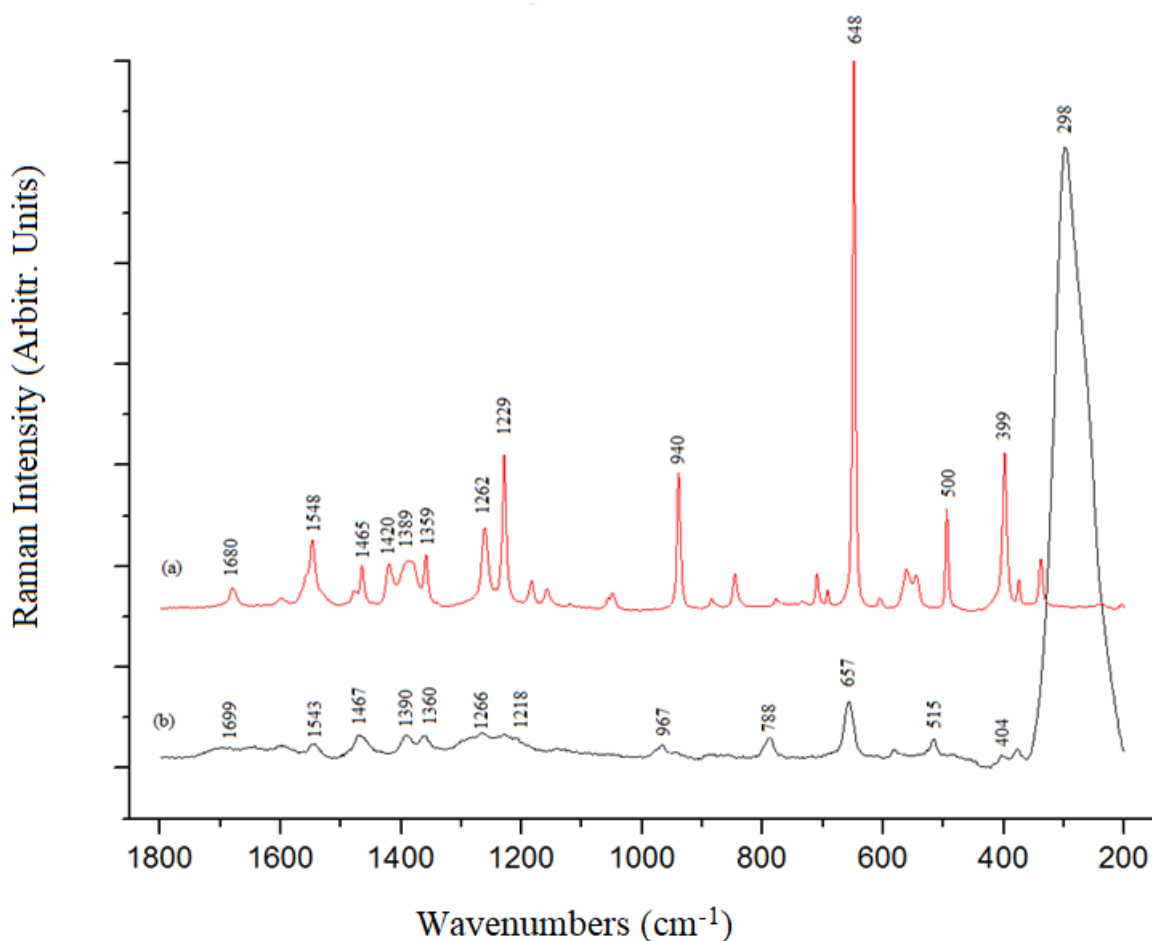


Figure 5 - Normal Raman spectrum (NRS) of solid Guanine (a) and SERS spectra of a 0.001 mol L^{-1} Guanine solutions acquired on a copper electrode at the OCP (b).

Table 2 – Wavenumbers and assignment for the main Raman bands of Guanine both in solid state and adsorbed on a copper electrode at the OCP.

Wavenumber (cm ⁻¹)		Assignment [27,28]
Solid	SERS E = -0.106 V	
-	298	ν_{CuCl}
399	404	$\delta_{\text{C2N10}} (\text{A}')$
500	515	$\delta_{\text{ring6}} (\text{A}')$
648	657	$\nu_{\text{ring6}} (\text{A}') + \omega_{\text{ring5}} (\text{A}'')$
940	967	$\delta_{\text{ring5}} (\text{A}')$
1229	1218	$\delta_{\text{C8H}}; \nu_{\text{C5N7-N7C8}} (\text{A}')$
1262	1266	$\nu_{\text{ring}}; \delta_{\text{C8H}}; \rho_{\text{NH2}} (\text{A}')$
1359	1360	$\delta_{\text{N1H}}; \delta_{\text{N10H12}}; \nu_{\text{C2N10}} (\text{A}')$
1389	1390	$\nu_{\text{ring5-N1C2}}; \delta_{\text{N9H}}; \delta_{\text{N1H}}; \rho_{\text{NH2}} (\text{A}')$
1420	-	$\delta_{\text{N9H}}; \nu_{\text{C8N9-N3C4+N1C2}} (\text{A}')$
1465	1467	$\nu_{\text{N7C8-N1C2-N3C4}}; \delta_{\text{C8H+N1H}} (\text{A}')$
1548	1543	$\nu_{\text{N3C4-C2N3+C2N10}}; \delta_{\text{NH2}}; \delta_{\text{N1H}} (\text{A}')$
1680	1699	$\nu_{\text{CO-C5C6}}; \delta_{\text{N1H}}; \delta_{\text{NH2}} (\text{A}')$

ν , ρ , δ and ω correspond to the stretching, rocking, in-plane, and out-of-plane angular deformation vibrational modes, respectively. A' and A'' are the symmetry species belonging to the C_s point group of the Guanine molecule.

Inhibition of X65 Steel Corrosion by Guanine

The electrochemical behavior of a X65 steel electrode immersed in either HCl 0.1 mol.dm⁻³ or Guanine 0.001 mol.dm⁻³ solutions, at pH = 2.0, was probed by cyclic voltammetry and the resulting cycles can be seen in Figure 6. It is possible to observe that the cycles obtained for the HCl solutions containing or not Guanine are quite similar, showing that this molecule is not able to modify the steel/solution interface to a significant extent. Indeed, both curves show a continuous increase in current density as the applied potential becomes more positive, showing that the iron is continually being dissolved as Fe^{+2} , which is the corrosion product expected for tested conditions, according to the Pourbaix diagram of the Fe/H₂O system [33]. The current density decreases gradually after the inversion potential ($E = +0.3$ V) until the OCP (-0.54 V) is reached. After that, the current density decreases again due to reduction of the H^+ ions until the end of the experiment, at $E = -1.0$ V. Addition of Guanine causes only a minor reduction of the maximum anodic current density, that drops from 67 mA.cm⁻² in blank solution's voltammogram to 62 mA.cm⁻² in the presence of the purine. Besides that, one can

see a small current plateau in the region between -0.5 and 0.7 V and a decrease in the current density observed at $E = -1.0$ V in the cathodic sweep of the cycle obtained for the Guanine solution, indicating that the purine makes the hydrogen evolution reaction a little more difficult to take place.

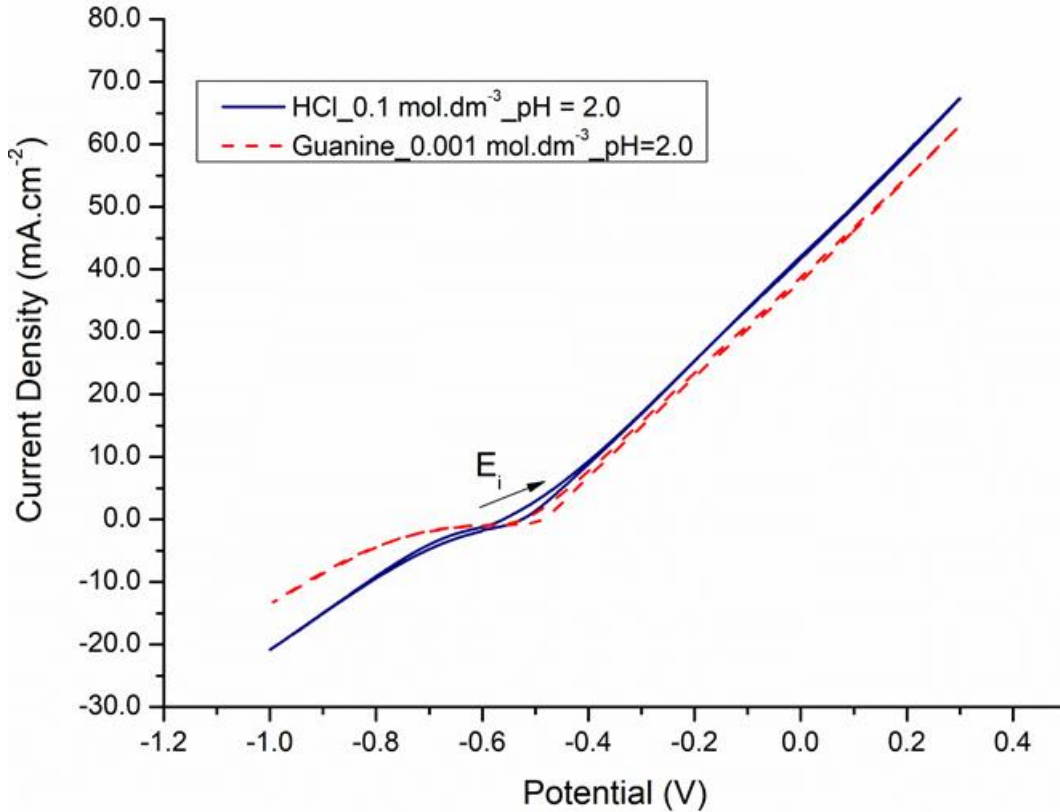


Figure 6 – Voltammograms of a X65 steel electrode immersed in neat HCl 0.1 mol.dm⁻³ (blue line) or Guanine 0.001 mol.dm⁻³ solutions (red line), at pH = 2.0.

Potentiodynamic polarization curves were also obtained for the X65 steel electrodes exposed to HCl solutions containing or not Guanine (Fig. 7). Once again, both curves are very similar, showing that Guanine could not influence either the anodic or the cathodic processes to a significant extent, confirming that the purine interacts very weakly with the metal surface, thus showing a quite low inhibition efficiency for the carbon steel in the tested conditions.

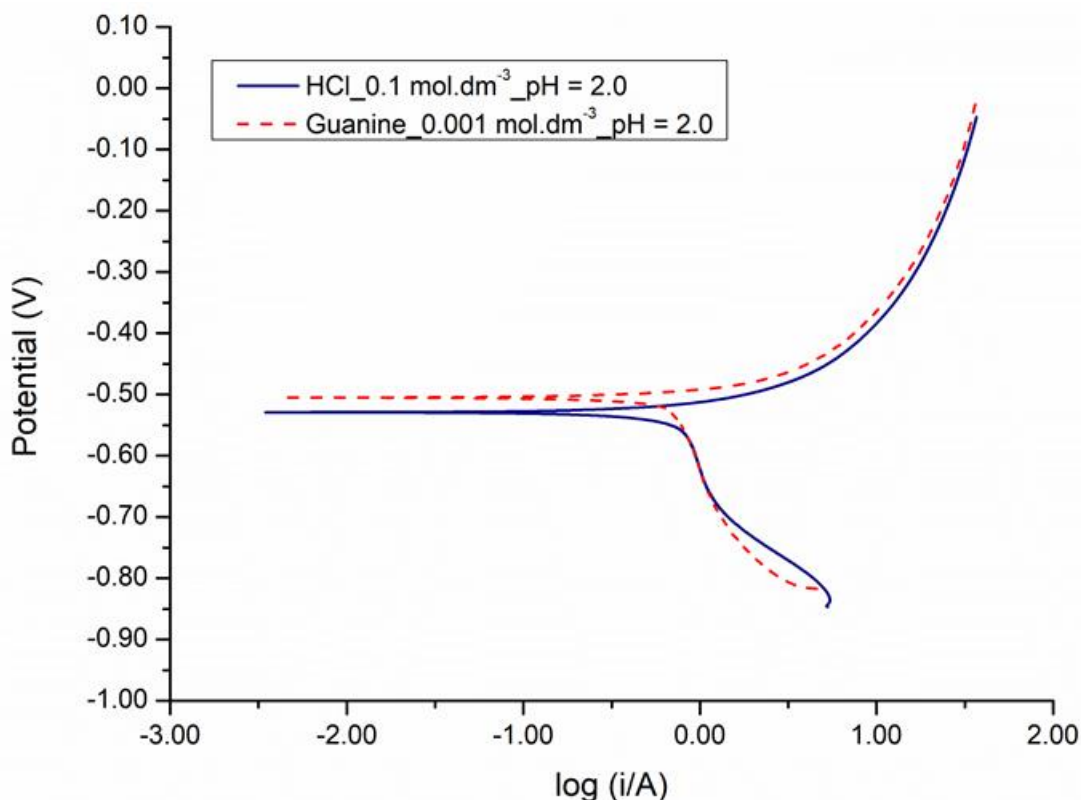


Figure 7 – Potentiodynamic polarization curves obtained for a X65 steel electrode immersed in either blank (blue line) or Guanine 0.001 mol.dm⁻³ (red line), pH = 2.0, solutions.

Weight loss experiments were carried out aiming at observing whether Guanine could show a better performance as a corrosion inhibitor for X65 steel in HCl medium at higher immersion times. The data obtained after 48 h of immersion are compiled in Table 3. These results corroborate the low IE of Guanine toward protection of the X65 steel in the tested condition, as anticipated by the electrochemical experiments, and reveal that its performance is not improved by a greater exposure time of the metal surface. It is worth mentioning that after the immersion test, the steel coupons were partially covered by a loose white product that resembled snowflakes. This compound fully detached from the metal surface during withdrawal of the solution and some of it could also be observed at the bottom of the flask where the experiment was conducted, showing that it has extremely low adhesion to the surface. Although characterization of this compound is yet to be carried out, the great amount of precipitate formed after immersion indicates that it is likely to be a reaction product of Guanine and iron and not simply excess Guanine that precipitated from the test solution.

Table 3 – Average weight loss calculated for X65 steel samples immersed for 90 h in HCl solutions (pH = 2.0) containing or not Guanine.

Solution	Weight loss/area (g.cm ⁻²)	Inhibition Efficiency (%)
HCl 0.1 mol.dm ⁻³	0.00856	-
Guanine 0.001 mol.dm ⁻³	0.00667	22

As mentioned before, iron cannot be considered as an appropriate SERS substrate in the conditions tested in this work, so acquiring in situ surface spectra of the X65 steel coupons is not possible, thus precluding a deeper analysis of the Guanine-iron specific interaction. However, it was possible to obtain Raman spectra from the bare steel surface after the weight loss experiment. A representative spectrum of the steel surface is shown in Figure 8, together with the Raman spectrum of solid Guanine. One can see that both spectra are nearly equal, showing that the neutral Guanine molecule can be found on the metal surface in detriment of the most abundant GuanineH⁺ species at pH = 2.0. Again, deprotonation of the cationic species takes place at the metal/solution interface, most likely due to a reduction of the pK_a for the deprotonation of GuanineH⁺ upon adsorption.

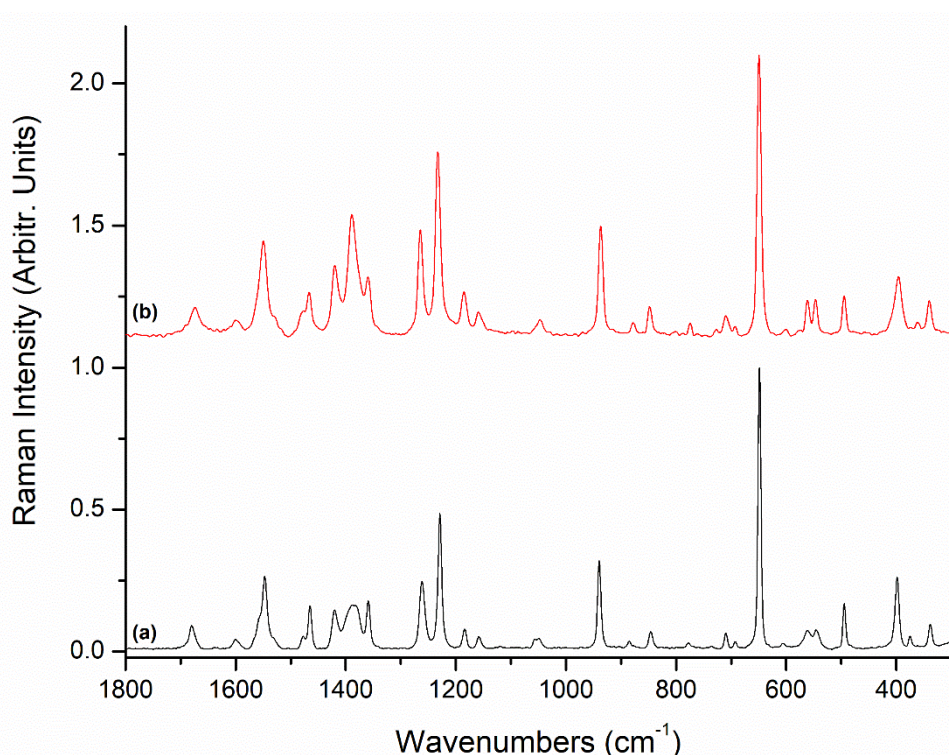


Figure 8 – Raman spectra of (a) solid Guanine and (b) the surface of a coupon obtained after the weight loss experiment.

At this point, a comparison of Guanine as an inhibitor for copper and X65 steel surfaces is in order. Even though neutral Guanine could be identified on both metal surfaces, the IE obtained for copper is much higher than the one calculated for the steel. Additionally, the reaction processes taking place at both interfaces are affected by the presence of Guanine at different extents, evidencing that the neutral molecule interacts with the metal surfaces in diverse ways, what ultimately reflects on the purine's ability to protect the different materials. Combined electrochemical, gravimetric and spectroscopic results revealed that chemisorption of Guanine onto copper is the first step to the formation of Cu(I)Guanine compound that eventually results in a continuous, thick and adherent film, effectively blocking the metal surface from further Cl⁻ attack and resulting in a high IE towards copper corrosion in HCl 0.1 mol.dm⁻³. Both electrochemical and weight loss results showed that Guanine is not able to modify the X65 steel surface significantly, so the corrosion processes continue with little interference from the purine. It could be argued that Guanine physisorbs on the steel surface in

the tested conditions and the absolute similarity between the solid Guanine Raman spectrum and that acquired after the weight loss experiment support this hypothesis, complementary techniques must be employed to elucidate it. Finally, Guanine may react with iron corrosion products to form an insoluble compound that is neither continuous nor adherent, and as such, it cannot provide any significant protection against corrosion of the X65 steel in the conditions used in this work.

Conclusion

Electrochemical, weight loss and Raman spectroscopic results showed that Guanine can efficiently inhibit copper corrosion in HCl 0.1 mol.dm⁻³ (pH = 2.0) by chemisorption of the neutral purine on the metal surface, that is followed by formation of Cu(I)Guanine insoluble compound. Such a compound forms an actual film at greater immersion times, that is uniform, continuous, and adherent, thus being able to protect the metal surface from significant attack of the aggressive species of the medium. A quite different behavior could be observed when X65 steel is immersed in the same test solution, where it could be seen that Guanine interacts weakly with the metal surface and eventually reacts with corrosion products to form a non-uniform and loose insoluble compound that cannot offer a significant degree of protection to the steel surface in the tested conditions. Characterization of the chemical composition and structure of both compounds are currently being carried out.

References

1. S. Papavinasam, "Corrosion Inhibitors", in: Uhlig's Corrosion Handbook, 3rd ed., Ed. R. W. Revie, John Wiley and Sons, New Jersey (2011) pp.1021-1032.
2. R. W. Revie and H. H. Uhlig, "Corrosion and Corrosion Control – An Introduction to Corrosion Science and Engineering", 4th ed., John Wiley and Sons, New Jersey (2008) pp. 303-316.
3. C. A. C. Sequeira, "Copper and Copper Alloys", in: Uhlig's Corrosion Handbook, 3rd ed., Ed. R. W. Revie, John Wiley and Sons, New Jersey (2011) pp.757-786.
4. M. C. Oliveira, R. M. Figueiredo, H. A. Acciari, E. N. Codaro, Journal of Materials Research and Technology, **7** (2018) 314.
5. A. Fateh, M. Aliofkhazraei, A. R. Rezvanian, Arabian Journal of Chemistry, **12** (2020) 481.
6. M. M. Antonijevic, M. B. Petrovic, International Journal of Electrochemical Society, **3** (2008) 1.
7. M. M. Antonijevic, M. B. Petrovic, International Journal of Electrochemical Society, **10** (2015) 1027.
8. C. Deslouis, B. Tribollet, G. Musiani, M. M. Musiani, Journal of Applied Electrochemistry, **18** (1988) 374.
9. C. Deslouis, B. Tribollet, G. Musiani, M. M. Musiani, Journal of Applied Electrochemistry, **18** (1988) 384.
10. C. J. Joia, R. F. Brito, B. C. Barbosa, F. D. Moraes, A. Z. Pereira, L. C. Marques, NACE International, 2011.
11. V. S. Sastri, "Green Corrosion Inhibitors: Theory and Practice", 1st ed., John Wiley and Sons, New Jersey (2011) pp. 257-303.
12. O. N. Eddy, M. Y. Habibat, E. E. Oguzie, Journal of Advanced Research, **6** (2015) 203.

13. Y. Yan, W. Li, L. Cai, B. Hou, *Electrochimica Acta*, **53** (2008) 5953.
14. H. F. Chahul, C. O. Akalezi, A. M. Ayuba, *International Journal of Chemical Science*, **7** (2015) 86.
15. Z. Tao, S. Wang, L. Ji, L. Zheng, W. He, *Advanced Materials Research*, **787** (2013) 30.
16. H. B. Singh, K. A. Bharati, *Handbook of Natural Dyes and Pigments*. Woodhead Publishing India, India, 2015.
17. T. Yamada, K. Shirasaka, A. Takano, M. Kawai, *Surface Science*, **561** (2004) 233.
18. M. Furukawa, T. Yamada, S. Katano, M. Kawai, H. Ogasawara, A. Nilsson. *Surface Science*, **601** (2007) 5433.
19. M. Furukawa, H. Tanaka, T. Kawai, *Journal of Chemical Physics*. **115** (2001) 3419.
20. E. F. Silva, J. S. Wysard, M. C. E. Bandeira, O. R. Mattos, *Corrosion Science*, submitted for publication.
21. ASTM, G 1-03. Standard Practice for Preparing, Cleaning, and Evaluating Corrosion Test Specimens,” Philadelphia, Pennsylvania: American Society for Testing and Materials, 2003.
22. E. F. Silva, M. C. E. Bandeira, W. A. Alves, O. R. Mattos, *Journal of the Electrochemical Society*, **165** (2018) C375.
23. E. F. Silva, J. S. Wysard, M. C. E. Bandeira, W. A. Alves, O. R. Mattos., *Journal of Raman Spectroscopy*, **50** (2019) 1438.
24. E. Le Ru, P. Etchegoin. “*Principles of Surface Enhanced Raman Spectroscopy*.”, 1st ed., Elsevier B. V. (2009), Oxford, pp. 121-183.
25. H. Gerengi, M. Mielniczek, G. Gece, M. M. Solomon, *Industrial and Engineering Chemistry Research*, **55** (2016) 9614.
26. H. Shiraishi, R. Takahashi, *Biochemistry and Bioenergetics*, **31** (1993) 203.
27. B. Giese, D. McNaughton, *Physical Chemistry Chemical Physics*, **4** (2002) 5161.
28. B. Giese, D. McNaughton, *Physical Chemistry Chemical Physics*, **4** (2002) 5171.
29. E. Koglin, J.-M. Séquaris, P. Valenta, *Journal of Molecular Structure*, **79** (1982) 185.
30. Darvishzad, T. Lubera, S. S. Kurek, *Journal of Physical Chemistry B*, **122** (2018) 7497.
31. W. S. Oh, M. S. Kim, S. W. Suh, *Journal of Raman Spectroscopy*, **17** (1987) 253.
32. L. E. Camafeita, S. Sánchez-Cortés, J. V. García-Ramos. *Journal of Raman Spectroscopy*, **27** (1996) 533.
33. V. Gentil, “Corrosão”, 3rd ed., Livros Técnicos e Científicos S. A. (1996), Rio de Janeiro, p. 25.